

Metaheuristic algorithm-based cascade PID controller design for fixed wing unmanned aerial vehicle

Mehmet Durmaz¹, Kenan Cici¹, Muhammet Sarıkaya¹, Mesut Bilici¹, Hasan Huseyin Bilgic^{1*}

¹Necmettin Erbakan University, Faculty of Aviation and Space Sciences, Aeronautical Engineering Department, Konya, 42140, Türkiye

Orcid: M. Durmaz (0000-0003-1145-7244), K. Cici (0000-0001-9211-4678), M. Sarıkaya (0000-0001-8217-1353), M. Bilici (0000-0002-0016-1600), H. H. Bilgic (0000-0001-6006-8056)

Abstract: In this study, the nonlinear model of the longitudinal and lateral motions of a fixed-wing Unmanned Aerial Vehicle (UAV) with assured geometrical features and aerodynamic parameters is linearized under certain conditions. A cascade proportional integral differential controller is designed on the linear model. The controller coefficients that applied to the model of the UAV were optimized with a metaheuristic algorithm, which is based on a metaheuristic search algorithm. The four different controller gains in the system are optimized using four different objective functions. Controller performances were tested in a simulation environment for unit step input responses. Considering the longitudinal dynamics of the aircraft, among the ITAE, ISE, MSE and IAE fitness functions, IAE can be shown as the optimum result for altitude control.

Keywords: Cascade PID, UAV, ABC Algorithm, Optimisation.

1. Introduction

Nowadays, when it comes to remotely controlled vehicles, the first thing that comes to mind is undoubtedly UAVs. Historically, UAVs were first used for military purposes. Tracking, surveillance and attack capabilities are among the most important features of UAVs according to their usage areas [1-4]. Compared to other aircraft, its costs are cheaper and easier to use, making it possible for civilians to use it as well. Therefore, using of UAVs has increased significantly, especially in areas such as search and rescue, logistics and real-time monitoring [5-6].

UAVs should provide certain features while performing their duties. Some of those features are high maneuverability, fast response of the system in case of any disturbance, high accuracy trajectory tracking, altitude control, etc. However, in order to meet these criteria, the controllers of the UAV must be reliable and respond quickly. Undoubtedly, the biggest challenge in controller design is the optimization process. Several methods have been derived for the optimization of the controller parameters used to obtain the properties that affect the performance, such as a fast response of the system, minimum steady-state error, minimum overshoot [7-9].

The control of fixed-wing UAVs has recently become a common subject of study. The absence of the human fac-

tor in it requires more trust in controllers while performing their duties. A reliable controller is critical to mission safety and cost. Route estimation and its planning are of vital importance for the unit to be tasked. In the literature, many solutions are presented to nonlinear equations and uncertainty situations in order to perform a task. In their study, Hervas et al. designed a nonlinear controller for the landing of a fixed-wing drone on the ship's deck with a Kalman filter using a scholastic downwind laser sensor. At the end of their studies, they showed that they gave successful results even at high angles of attack [10]. Autopilot design using a controller is widely used, especially in small-sized and commercial fixed-wing unmanned aerial vehicles. Stastny et al. applied speed and path control to a small model unmanned aerial vehicle with a 'high level Nonlinear Model Predictive Controller'. As a result of their work, predicts that are quite similar to simulation answers and real-time answers have been provided [11]. Yan and Wang, on the other hand, designed a 'low gain' controller for swarm UAVs and made speed control [12]. Zhen et al. compared 'the trained reinforcement learning (RL)' controller designed for a fixed-wing UAV with a Proportional-Integral-Derivative (PID) controller. They showed that RL gives better results in the simulations than PID in disturbances, such as wind and turbulence. They also stated that PID gains should be tuned according to different flight conditions [13]. Poksawat et

* Corresponding author.
Email: hhbilgic@erbakan.edu.tr



al. designed a ‘gain scheduled’ controller for a fixed-wing mini-UAV. They tested the PID coefficients according to different conditions by measuring the instantaneous velocity with a Pitot tube. The results were validated in the wind tunnel under different conditions. As a result, they revealed that their proposed method creates less deviation in height compared to the traditional method [14]. Mammarella et al. designed an autopilot for a nonlinear model using the ‘sample-based stochastic model predictive control (SMPC)’ method. They performed a traction control of a mini UAV and verified it with simulations. As a result, they stated that the SMPC architecture is less affected by disturbances than the classical Model Predictive Control (MPC) architecture [15].

In this study, the longitudinal PID controller parameters applied to the dynamically modeled fixed-wing unmanned aerial vehicle were optimized with the metaheuristic search algorithm. The nonlinear RQ-2 Pioneer model, which was modeled mathematically, was linearized, and the controller was designed under certain trim conditions. Tuning of PID parameters of multi-degree-of-freedom systems takes a long time with trial and error methods. In most cases, the desired results are not achieved. For this reason, ABC optimization, one of the metaheuristic algorithms, is proposed in this study. In the PID controller design, the PID parameters for the control of each of the UAV’s pitch speed, pitch angle, altitude and true air speed (TAS) were found with the Artificial Bee Colony (ABC) approach, which is a metaheuristic search algorithm technique. The reason for this can be shown as the poor performance of traditional tuning methods when the systems are not linear [16]. With the development of metaheuristic algorithms, their use in controller design has become widespread and has become more efficient to find the optimum PID parameter values [17].

In section 2, the introduction of fixed-wing UAVs and metaheuristic search algorithms are mentioned under the title of materials and methods. Research findings, algorithm block diagram and system response for objective function are presented in section 3. Finally, in section 4, the results of the system output are interpreted and discussed.

2. Materials and Methods

2.1. AAI RQ-2 Pioneer Fixed Wing Unmanned Aerial Vehicle

The RQ-2 Pioneer is an unmanned aerial vehicle used at sea and on land from 1986 to 2007 by the United States Navy, Marine Corps and Army. Initially placed on Iowa-class battleships to provide artillery detection, its mission has evolved primarily into reconnaissance and surveillance for amphibious forces. In addition to this, many experimental and academic studies have been done on it in the literature [18]. Aerodynamic coefficients, mass and geometric properties taken from the wind tunnel test in Robert Bray’s master’s thesis, which is one of these

studies, were used in this study [19]. Table 1 presents the technical specifications of the AAI RQ-2 Pioneer.

Table 1. Specifications of AAI RQ-2 Pioneer [19]

Property	Description	Value	Unit
I_x	Moment of Inertia along X_B axis	47.2258	kgm^2
I_y	Moment of Inertia along Y_B axis	90.9482	kgm^2
I_z	Moment of Inertia along Z_B axis	111.4753	kgm^2
I_{xy}	Product of Inertia along $X_B Y_B$ axis	0.0	kgm^2
I_{xz}	Product of Inertia along $X_B Z_B$ axis	-6.6462	kgm^2
I_{yz}	Product of Inertia along $Y_B Z_B$ axis	0.0	kgm^2
S	Wing area	2.8261	m^2
\bar{c}	Mean aerodynamic chord	0.54864	m
b	Wing span	5.15	m
m	Mass of UAV	190.5088	kg

2.2. Dynamic Model of AAI RQ-2 UAV

Creating a dynamic model of the aircraft is quite complex. Therefore, some assumptions have been made. These are given below [20].

- The UAV is considered a rigid body.
- The inertial mass of UAVs is constant and is the initial flight state value.
- The UAV has a constant gravitational acceleration.
- The Earth is treated as a stationary plane in inertial space.
- The angular momentum changes due to rotating subsystems are neglected.
- The angular momentum changes due to fuel sloshing, the motion of hinged parts and elastic deformation are neglected.

Newton’s 2nd law is applied by taking the above assumptions [20].

$$F_t = m \frac{d(v)}{dt} \tag{1}$$

$$G_t = \frac{d(h)}{dt} \tag{2}$$

F_t , G_t and h are the total external force, total external moment and angular momentum respectively

$$h_B = I_B \omega_B \tag{3}$$

I_B and ω_B are moment of inertia and angular momentum, respectively. In this case, the two products of inertia, I_{xv} and I_{vz} are zero.

$$I_B = \begin{bmatrix} I_x & -I_{xy} & -I_{xz} \\ -I_{xy} & I_y & -I_{yz} \\ -I_{xz} & I_{zy} & I_z \end{bmatrix}$$

$$I_B = \begin{bmatrix} I_x & -I_{xy} & -I_{xz} \\ -I_{xy} & I_y & -I_{yz} \\ -I_{zx} & I_{zy} & I_z \end{bmatrix} \quad \text{and}$$

$$\omega_B = [p \quad q \quad r]^T \quad (4)$$

B subscript indicates the body fixed frame those vectors describe on them. The nonlinear equations are attained by utilizing Newton's second law and the assumptions.

$$X - mg \sin \theta = m(\dot{u} + qw - rv) \quad (5)$$

$$Y - mg \cos \theta \sin \phi = m(\dot{v} + ru - pw) \quad (6)$$

$$Z - mg \cos \theta \cos \phi = m(\dot{w} + pv - qu) \quad (7)$$

$$L = I_x \dot{p} - I_{zx} \dot{r} + qr(I_z - I_y) - I_{zx} pq \quad (8)$$

$$M = I_y \dot{q} + rp(I_x - I_z) - I_{zx}(p^2 - r^2) \quad (9)$$

$$N = I_x \dot{r} - I_{zx} \dot{p} + pq(I_y - I_x) - I_{zx} qr \quad (10)$$

$$p = \dot{\phi} \sin \theta \quad (11)$$

$$q = \dot{\phi} \cos \theta \sin \phi + \dot{\theta} \cos \phi \quad (12)$$

$$r = \dot{\phi} \cos \theta \cos \phi - \dot{\theta} \sin \phi \quad (13)$$

$$\phi = p + (q \sin \theta + r \cos \theta) \tan \theta \quad (14)$$

$$\theta = q \cos \phi - r \sin \phi \quad (15)$$

$$\dot{\phi} = (q \sin \theta + r \cos \theta) \sec \theta \quad (16)$$

$$\dot{x}_E = u^E \cos \theta \cos \phi + v^E (\sin \theta \sin \phi \cos \phi - \cos \theta \sin \phi) + w^E (\cos \theta \sin \phi \cos \phi - \sin \theta \sin \phi) \quad (17)$$

$$\dot{y}_E = u^E \cos \theta \sin \phi + v^E (\sin \theta \sin \phi \sin \phi - \cos \theta \cos \phi) + w^E (\cos \theta \sin \phi \sin \phi - \sin \theta \cos \phi) \quad (18)$$

$$\dot{z}_E = -u^E \sin \theta + v^E \sin \theta \cos \theta + w^E \cos \theta \cos \theta \quad (19)$$

$$u^E = u + W_x \quad (20)$$

$$v^E = v + W_y \quad (21)$$

$$w^E = w + W_z \quad (22)$$

15 nonlinear ordinary differential equations in the independent variable time (t) and three algebraic equations are obtained. 3 of the differential equations are not independent, thus there are 12 independent equations.

X , Y , and Z represent aerodynamic forces, and L , M and N are moments components of UAV on the body axes. Moments and forces depend on linear velocities (u , v , w), angular velocities (p , q , r), and one control vector.

2.3. PID Controller Design

PID controller stands for Proportional-Integral-Derivative and regulates different parameters, such as pressure, temperature and speed at desired values. As in many sectors, its use in aviation is quite common. As in this study, it was used in aircraft for longitudinal motion (altitude and velocity) control. In systems with PID controller feedback, the error value of the output signal is calculated

according to the input signal, and the cycle continues until this value is minimum.

Proportional-Integral-Derivative controllers each contain advantages and disadvantages. The purpose of the PID controller is to complete the deficiency of each other by using three controllers simultaneously. The PID controller provides a reasonable system response by eliminating the steady state error and reducing the settlement time. The PID controller equation used in the study is presented with equation 23.

$$u(t) = Kp e(t) + Kd \frac{e(t)}{dt} + Ki \int e(t) dt \quad (23)$$

Today, the advanced version of the classical PID control systems with feedback is the cascade control structure, which can also be applied to multi-degree-of-freedom systems [21-23]. Cascade controller structure, in short, means that a control variable is controlled gradually when there is more than one measurement. In the cascade control system, first, the parameters of the inner loop controller are determined and then the parameters of the outer loop controller are obtained [24]. A metaheuristic algorithm-based search algorithm was used to find internal and external controller parameters simultaneously in this study.

2.4. Artificial Bee Colony Algorithm

Metaheuristic algorithms are defined by several different classes according to their characteristic structures. In one of these classes, the bio-inspired metaheuristic algorithm, as the name suggests, is a form of optimization created by examining the life instincts of various living things based on swarm intelligence, such as humans, animals, cells, etc. There are various variations, such as particle swarm optimization, ant colony optimization, Artificial Bee Colony optimization, bat algorithm optimization, etc. [25-26]. The Artificial Bee Colony search algorithm used in this article was first introduced by Karaboğa in 2005 by making an analogy with honey bees based on their foraging instincts [27].

The ABC algorithm model consists of three groups of bees. The first group, the worker bee group, looks for productive food sources around the hive and is responsible for keeping their location and nectar information in mind and conveying them to the other bees in the hive with a 'waggle dance' in the dance area. Onlooker bees, following the information brought by the worker bees in the dance area, try to determine the most efficient food source in direct proportion to the productivity with the 'greedy selection' method [28]. As a result of this selection, the scouts gravitate towards productive food sources. Only one worker bee or onlooker bee is assigned for each food source. Worker bees, found in other food sources that are insufficient, leave the food source they have exploited and turn into scout bees and disperse in the search space to find more efficient food sources. When applied to real-life problems, nectar productivity in food sources represents the optimized system. The implementation of this algorithm becomes an iterative

process that continues until the requirements of system optimization are achieved. This iterative cycle continues until the most efficient resource is found, and system performance is improved [27]. Figure 1 presents the flowchart of the ABC algorithm.

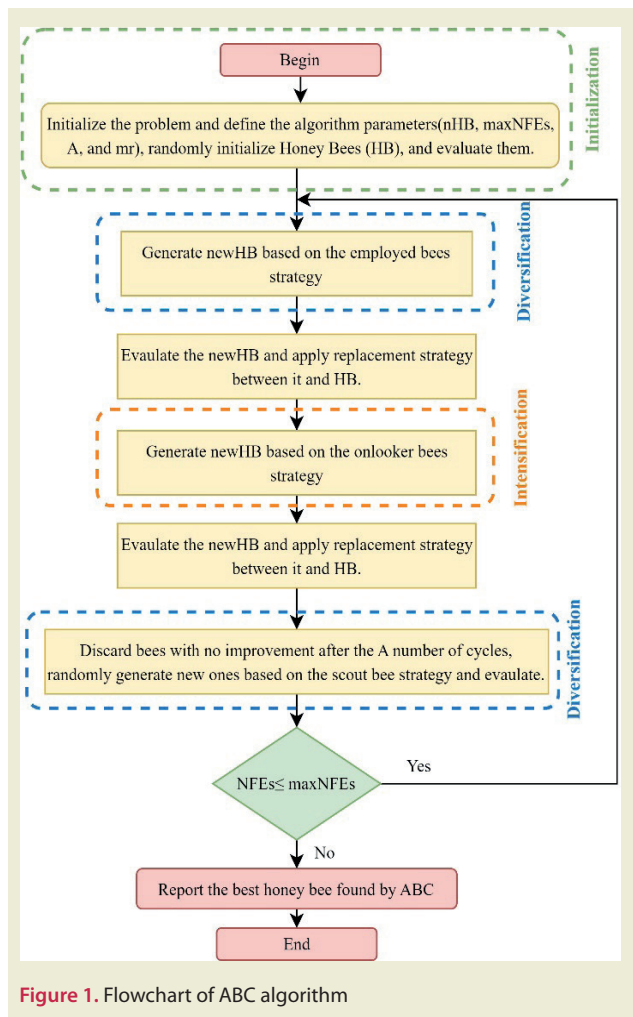


Figure 1. Flowchart of ABC algorithm

3. Results and Discussion

6 DOF model and 3 DOF control of the Pioneer RQ-2 UAV were created in the Matlab/Simulink environment. The flow diagram of the control system is shown in Figure 2.

As seen in the Figure 2, the altitude, speed, pitch angle and pitch rate values are controlled with a cascade structure. Controller parameters are optimized with the ABC algorithm. During the optimization process, four different fitness functions were used. The designed objective

All objective functions successfully followed the 450 meters altitude requirements, which were given as step input to the 5th second of the flight simulation. Among the answers, the objective function with the least oscillation, overshoot and least steady-state error was found to be IAE. Also, IAE is almost as successful as ITAE when the UAV’s pitch angle increased for the desired altitude

functions consist of MSE (Mean Square Error), ITAE (Integral Time Absolute Error), ISE (Integral Square Error) and IAE (Integral Absolute Error) fitness functions that are frequently used in the literature [29-31]. The determined objective functions are presented in equations 28-31.

$$error_h = Altitude_{ref} - Altitude \tag{24}$$

$$error_\theta = Theta_{ref} - Theta \tag{25}$$

$$error_q = q_{ref} - q \tag{26}$$

$$error_{TAS} = TAS_{ref} - TAS \tag{27}$$

$$J_{ISE} = \sum_{t=0}^{40} error_h(t)^2 + error_\theta(t)^2 + error_q(t)^2 + error_{TAS}(t)^2 \tag{28}$$

$$J_{IAE} = \sum_{t=0}^{40} |error_h(t)| + |error_\theta(t)| + |error_q(t)| + |error_{TAS}(t)| \tag{29}$$

$$J_{ITAE} = \sum_{t=0}^{40} t (|error_h(t)| + |error_\theta(t)| + |error_q(t)| + |error_{TAS}(t)|) \tag{30}$$

$$J_{MSE} = \frac{1}{40} \sum_{t=0}^{40} t (error_h(t)^2 + error_\theta(t)^2 + error_q(t)^2 + error_{TAS}(t)^2) \tag{31}$$

The optimization process consisting of a maximum of 100 iterations and 40 seconds was performed for the four objective functions. The scatter graphs obtained are presented in Figure 3.

For each algorithm, the lower and upper limits of the PID gains were selected the same, and the optimization process was carried out for the same conditions. The best PID coefficients found for each objective function are given in Table 2.

The performance analyzes of the controllers designed with different objective functions were evaluated for 40 seconds during the cruise flight at 100 meters altitude, and the results are shown in Figure 4.

response. Additionally, all aircraft have a pitch rate limit. Sudden changes in the control surface increase the load on the hinge point of the elevator and strained the entire control surface system. For this reason, the pitch rate of the UAV could not provide as good a result as the altitude and pitch angle against the 450 meters altitude requirements. Notwithstanding, it has been found the best gains

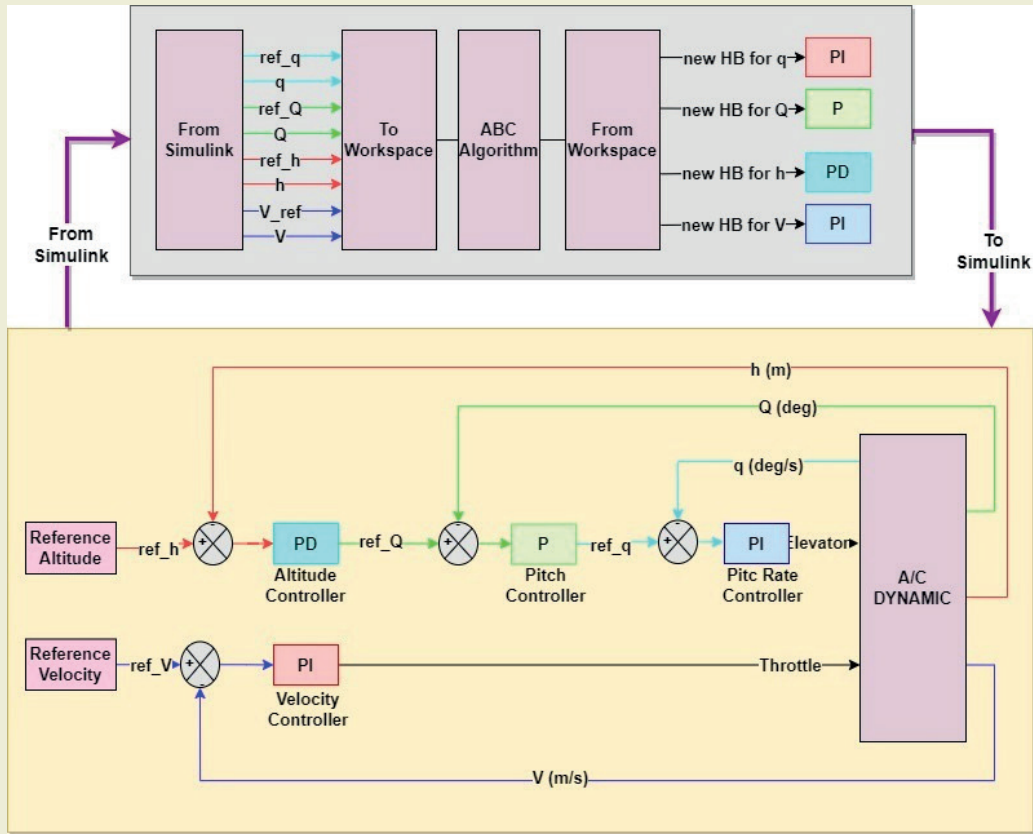


Figure 2. Cascade PID Control Flow Diagram

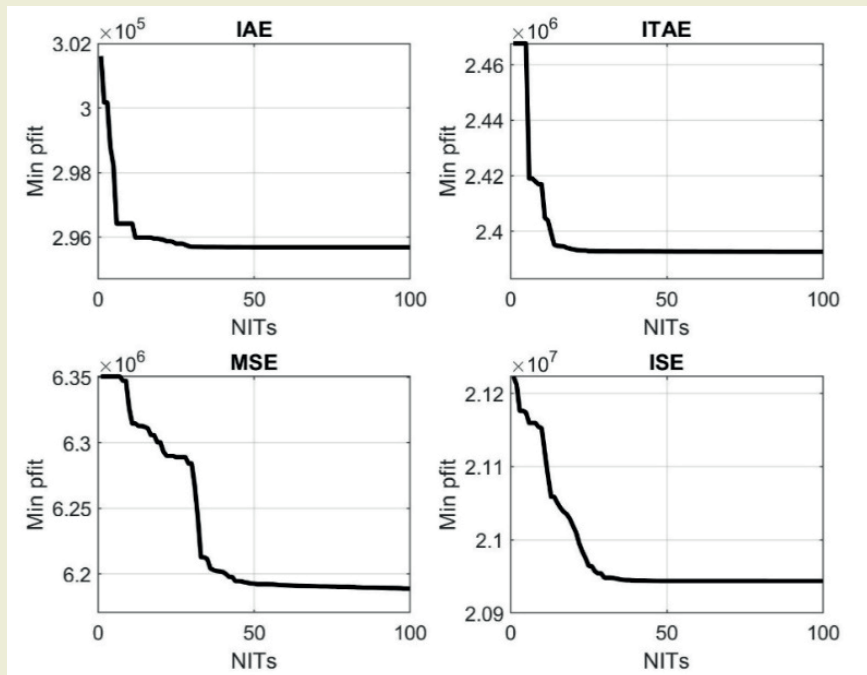


Figure 3. Scatter graphs for IAE, ITAE, MSE and ISE Objective Functions

Table 2. PID Gains of Objective Functions

	Pitch Rate		Theta	Altitude		TAS	
	P	I	P	P	D	P	I
J_{ISE}	-1	-36.384	1.42292	1.033536	0.522843	0	200
J_{IAE}	-50	-200	1.573113	1.990487	1.618973	195.4142	200
J_{ITAE}	-1.71825	-1	1.321292	1.340334	1.276471	199.7004	198.5689
J_{MSE}	-49.9994	-200	14.37209	1.96579	0.760183	195.4503	199.9767

that give the most stable response for pitch rate. Finally, the objective function that makes the least change for the true airspeed (TAS) of the UAV is prescribed as MSE. True airspeeds for all objective functions show that varied with low intervals.

The time response characteristics of the designed control system are presented in Table 3. According to these results, while the objective function with the lowest overshoot was J_{IAE} , the objective function with the lowest settling time was J_{MSE} . Although all objective functions exhibit successful system behavior, J_{IAE} stands out with these features, especially since the overshoot and peak values are expected to be low in the pitching movements of UAVs.

In spite of altitude requirements and responses, there is

no reference input for speed and the UAV tends to maintain its true airspeed. For any altitude input, a change in velocity will occur, as kinetic energy will momentarily transform into potential energy. However, this change is brought closer to the equilibrium state by the speed controller. The closer this speed is to the trim speed, the better the velocity controller is. Therefore, the best result for cruise true airspeed is seen as the J_{MSE} objective function.

4. Conclusion

In this study, the nonlinear model of an unmanned aerial vehicle was linearized, and the longitudinal controller was designed on the linear model. In the controller design, besides the altitude control of the UAV, the speed control is also performed using a cascade PID controller. Seven gains of four different controllers are optimized

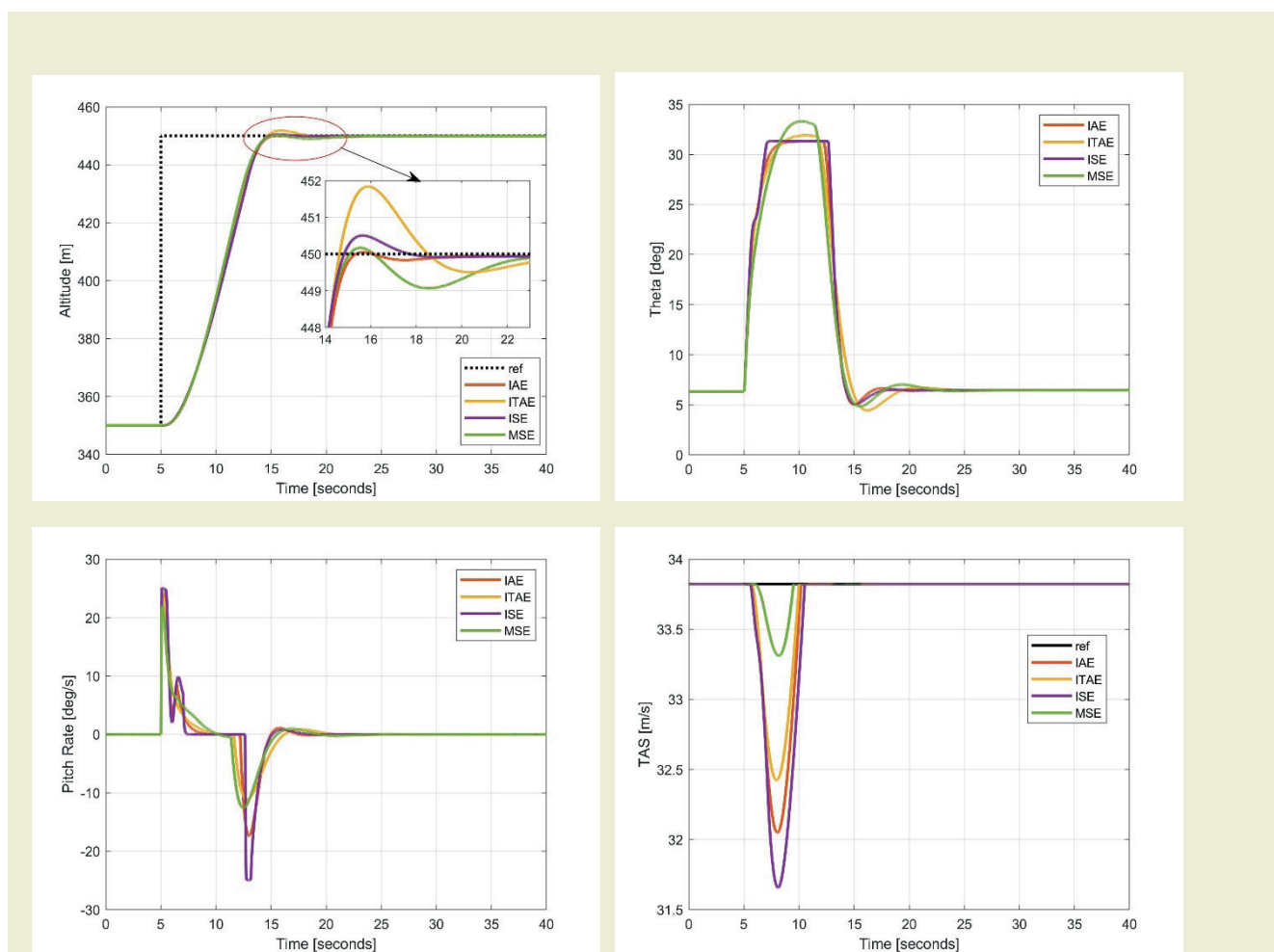


Figure 4. System Responses of a) Altitude b) Theta c) Pitch Rate d) TAS (True Air Speed)

Table 3. Time domain specifications.

	Rise Time	Settling Time	Settling Min	Settling Max	Overshoot	Undershoot	Peak	Peak Time
J_{ISE}	5.935	14.243	440.001	451.989	0.44	0	452	15.986
J_{IAE}	5.880	14.252	440.016	450.047	0.01	0	450	15.66
J_{ITAE}	5.881	14.163	440.021	450.503	0.11	0	450.5	15.642
J_{MSE}	5.632	14.153	440.002	450.169	0.04	0	450.2	15.538

with the ABC algorithm. In the optimization process, ITAE, ISE, MSE and IAE functions are used in the design of the objective function, which are the fitness functions whose effectiveness has been proven in the literature. Objective function; It is created with the fitness functions of altitude, pitch angle, pitch rate, and true airspeed. The system responses obtained as a result of the optimization are presented with tables and graphics. When the results were examined, it was revealed that the longitudinal con-

trol of the UAV gave the best result, with a 0.01 maximum overshoot of the J_{IAE} objective function. It is foreseen that the proposed optimization approach can be a guide in the control of multi-degree-of-freedom systems.

5. Conflict of Interest

The authors declare that there is no conflict of interest regarding the publication of this paper.

References

- [1] Han, T., Xiao, B., Zhan, X. S., Wu, J., & Gao, H. (2019). Time-optimal control of multiple unmanned aerial vehicles with human control input. *International Journal of Intelligent Computing and Cybernetics*, 12(1), 138-152.
- [2] Alladi, T., Chamola, V., & Kumar, N. (2020). PARTH: A two-stage lightweight mutual authentication protocol for UAV surveillance networks. *Computer Communications*, 160, 81-90.
- [3] Xia, C., Yongtai, L., Liyuan, Y., & Lijie, Q. (2020). Cooperative task assignment and track planning for multi-UAV attack mobile targets. *Journal of Intelligent & Robotic Systems*, 100(3), 1383-1400.
- [4] Bilici, M., Karılı, M., (2022) Modeling and Control of a Fixed-Wing High-Speed UAV. *International Journal of Aviation Science and Technology*, 3(01), 35-44.
- [5] Altan, A. (2020, October). Performance of metaheuristic optimization algorithms based on swarm intelligence in attitude and altitude control of unmanned aerial vehicle for path following. In *2020 4th International Symposium on Multidisciplinary Studies and Innovative Technologies (ISMSIT)* (pp. 1-6). IEEE.
- [6] Ilango, H. S., & Ramanathan, R. (2020). A Performance Study of Bio-Inspired Algorithms in Autonomous Landing of Unmanned Aerial Vehicle. *Procedia Computer Science*, 171, 1449-1458.
- [7] Mobarez, E. N., Sarhan, A., & Ashry, M. M. (2019, December). Robust PID Flight Controller for Ultrastick-25e UAV. In *2019 15th International Computer Engineering Conference (ICENCO)* (pp. 150-156). IEEE.
- [8] Kaba, A. (2021). Improved PID rate control of a quadrotor with a convexity-based surrogated model. *Aircraft Engineering and Aerospace Technology*. 93, 1287–1301.
- [9] Amarat, S. B., & Zong, P. (2019). 3D path planning, routing algorithms and routing protocols for unmanned air vehicles: a review. *Aircraft engineering and aerospace technology*.
- [10] Hervas, J. R., Reyhanoglu, M., Tang, H., & Kayacan, E. (2016). Nonlinear control of fixed-wing UAVs in presence of stochastic winds. *Communications in Nonlinear Science and Numerical Simulation*, 33, 57-69.
- [11] Stastny, T., & Siegart, R. (2018, June). Nonlinear model predictive guidance for fixed-wing UAVs using identified control augmented dynamics. In *2018 International Conference on Unmanned Aircraft Systems (ICUAS)* (pp. 432-442). IEEE.
- [12] Yan, J., Yu, Y., & Wang, X. (2022). Distance-based formation control for fixed-wing UAVs with input constraints: A low gain method. *Drones*, 6(7), 159.
- [13] Zhen, Y., Hao, M., & Sun, W. (2020, November). Deep reinforcement learning attitude control of fixed-wing UAVs. In *2020 3rd International Conference on Unmanned Systems (ICUS)* (pp. 239-244). IEEE.
- [14] Poksawat, P., Wang, L., & Mohamed, A. (2017). Gain scheduled attitude control of fixed-wing UAV with automatic controller tuning. *IEEE Transactions on Control Systems Technology*, 26(4), 1192-1203.
- [15] Mammarella, M., Capello, E., Dabbene, F., & Guglieri, G. (2018). Sample-based S MPC for tracking control of fixed-wing UAV. *IEEE control systems letters*, 2(4), 611-616.
- [16] Abachizadeh, M., Yazdi, M. R. H., & Yousefi-Koma, A. (2010, July). Optimal tuning of PID controllers using artificial bee colony algorithm. In *2010 IEEE/ASME International Conference on Advanced Intelligent Mechatronics* (pp. 379-384). IEEE.
- [17] Coban, S., Bilgic, H.H., Akan, E. (2020). Improving autonomous performance of a passive morphing fixed wing UAV. *Informaton Technology and Control*. 49 (1), pp. 28-35.
- [18] McCafferty, J. P., Woodward, D. A., Ray, G., Bachelani, A., & Kim, B. (2014). Investigation of an autonomous landing sensor for unmanned aerial systems. In *AIAA Guidance, Navigation, and Control Conference* (p. 0979).
- [19] Bray, R. M. (1991). A wind tunnel study of the Pioneer remotely piloted vehicle. *NAVAL POSTGRADUATE SCHOOL, MONTE-REY CA*.
- [20] Etkin, B., & Reid, L. D. (1995). *Dynamics of flight: stability and control*. John Wiley & Sons.
- [21] Johnson, M. A., & Moradi, M. H. (2005). *PID control*. London, UK: Springer-Verlag London Limited.
- [22] Kada, B., & Ghazzawi, Y. (2011, October). Robust PID controller design for an UAV flight control system. In *Proceedings of the World congress on Engineering and Computer Science* (Vol. 2, No. 1-6, pp. 1-6).
- [23] Andrade, F. A., Guedes, I. P., Carvalho, G. F., Zachi, A. R., Haddad, D. B., Almeida, L. F., ... & Pinto, M. F. (2021). Unmanned Aerial Vehicles Motion Control with Fuzzy Tuning of Cascaded-PID Gains. *Machines*, 10(1), 12.
- [24] Bilgiç, H. H., Tutumlu, M. S., & Conker, Ç. (2021). Top ve çubuk sistemi için kaskad denetleyici parametrelerinin meta-sezgisel algoritmalarla optimizasyonu. *Dokuz Eylül Üniversitesi Mühendislik Fakültesi Fen ve Mühendislik Dergisi*, 23(67), 157-167.
- [25] Bilgic, H. H., Sen, M. A., Yapici, A., Yavuz, H., & Kalyoncu, M. (2021). Meta-heuristic tuning of the LQR weighting matrices using various objective functions on an experimental flexible arm under the effects of disturbance. *Arabian Journal for Science and Engineering*, 46(8), 7323-7336.
- [26] Guvenc, M. A., Bilgic, H. H., Cakir, M., & Mistikoglu, S. (2022). The prediction of surface roughness and tool vibration by using metaheuristic-based ANFIS during dry turning of Al alloy (AA6013). *Journal of the Brazilian Society of Mechanical Sciences and Engineering*, 44(10), 1-14.
- [27] Karaboga, D. (2005). An idea based on honey bee swarm for

- numerical optimization (Vol. 200, pp. 1-10). Technical report-tr06, Erciyes university, engineering faculty, computer engineering department.
- [28] Akay, B., & Karaboga, D. (2012). Artificial bee colony algorithm for large-scale problems and engineering design optimization. *Journal of intelligent manufacturing*, 23(4), 1001-1014.
- [29] Hekimoğlu, B. (2019). Optimal tuning of fractional order PID controller for DC motor speed control via chaotic atom search optimization algorithm. *IEEE Access*, 7, 38100-38114.
- [30] Shagor, M. R. K., Nishat, M. M., Faisal, F., Mithun, M. H., & Khan, M. A. (2021, December). Firefly algorithm based optimized PID controller for stability analysis of DC-DC SEPIC converter. In 2021 IEEE 12th Annual Ubiquitous Computing, Electronics & Mobile Communication Conference (UEMCON) (pp. 0957-0963). IEEE.
- [31] Maghfiroh, H., Saputro, J. S., Hermanu, C., Ibrahim, M. H., & Sujono, A. (2021, March). Performance Evaluation of Different Objective Function in PID Tuned by PSO in DC-Motor Speed Control. In *IOP Conference Series: Materials Science and Engineering* (Vol. 1096, No. 1, p. 012061). IOP Publishing.